



Lung Cancer Prediction and Classification Using Deep Learning Techniques

Ms. Shilpa¹, A Tejashwini²

*1 Assistant Professor, Department of CSE, Malla Reddy College of Engineering for Women.,
Maisammaguda., Medchal., TS, India*

2, B.Tech CSE (20RG1A0564),

Malla Reddy College of Engineering for Women., Maisammaguda., Medchal., TS, India

Abstract

The substantial health risk posed by lung cancer has sparked general public alarm. The likelihood of a favourable outcome from therapy for lung cancer is greatly improved by early identification. One potential way to improve the accuracy of early-stage lung cancer detection is to use deep learning in conjunction with a convolutional neural network (CNN). Using data sets obtained from the Image Database Resource Initiative (IDRI) and the Lung Image Database Consortium (LIDC), this research presents two separate approaches to lung cancer detection. Support vector machines (SVMs) and deep convolutional neural networks (CNNs) are used to classify lung cancer images as either malignant or non-cancerous. The convolutional neural network (CNN) is trained in MATLAB using either a single batch or numerous batches before classification. During multiple batch training, the deep CNN achieves an accuracy of 80% and during single batch training, it achieves a surprising 100% in classification, which is a huge improvement over the SVM's modest 65%. The remarkable testing performance of the deep CNN stands out; in less than 20 iterations, it achieves nearly 100% classification accuracy. The assessment is carried out with the use of 25 CT scans of the lungs, with a resolution of 512×512 pixels each scan. In contrast to earlier studies that mostly concentrated on clipped pictures of lung cancer nodules, this one demonstrates the effectiveness of the deep CNN in evaluating complete lung CT scans.

INTRODUCTION

Undoubtedly, lung cancer stands as the leading cause of cancer-related deaths in both men and women, surpassing the combined mortality rates of breast, colon, and prostate cancers. According to the American Society of Lung Cancer, approximately 609,360 deaths and 1,918,030 new diagnoses of lung cancer were reported in the US last year alone[1]. Lung cancer constitutes 5.9% of India's total cancer cases, totalling 5.26 million. Despite its severity, some cases of lung cancer are treatable, with around 350,000 individuals surviving after early detection and treatment. Hence, early detection is crucial for enhancing patients' chances of recovery.

Several invasive methods exist for detecting lung cancer, such as spiral computed tomography, sputum cytology, fluorescence bronchoscopy, and lung cancer-related antigens. However, their efficacy is limited compared to previous detection techniques. Notably, the support vector machine (SVM) classifier demonstrated superior effectiveness in tests



involving rice, data mining, and skin disease diagnosis. Additionally, reports from [7] to [11] detail CNN training for medical image categorization, while [12] to [14] document the utilization of CNNs and other deep learning models for diagnosing lung cancer following unsupervised pretraining on medical or natural imagery. Furthermore, Barbu et al. [13] and Feulner et al. [17] provide detailed reports on the extraction of multi-level image characteristics for detecting lung nodules and the subsequent analysis results.

Utilizing deep learning techniques alongside a voting function, Rossetto et al. [20] achieved a remarkable accuracy rate of 97.5% in classifying lung cancer, with a false positive rate of less than 10%. Conversely, manual sputum sample analysis, although prone to errors and time-consuming, necessitates skilled individuals to mitigate mistakes [21]. In a study by Wu and Zhao, their supervised machine learning system, based on entropy degradation and tested on a limited set of computed tomography (CT) lung images, attained a lung cancer detection accuracy of 77.8% [12]. Kaur [3] presents a survey on various Lung Cancer Detection techniques, while Taher and Sammouda's research focuses on early-stage lung cancer detection through color sputum image analysis employing neural networks (NN) and a fuzzy c-mean (FCM) clustering algorithm [24]. Intel's examination of cervical cancer detection revealed an 81% accuracy enhancement with deep learning (DL) technology [25].

According to Turkki et al. [26], deep convolutional neural networks (CNN) achieved an F-score of 0.94 in quantifying areas within samples stained with hematoxylin and eosin, containing numerous immune cells. An annotation procedure guided by antibodies expedited this process. Shin et al.'s investigation involved transfer learning-based CNN for lymph node (LN) detection in the thoraco-abdominal region and classification of interstitial lung disease (ILD). Their study on mediastinal LN identification using axial CT slices alongside ILD categorization achieved 85% sensitivity with a false positive rate of 3% [27]. Utilizing the LIDC-IDRI dataset, Krewer et al. [28] examined lung cancer detection and attained a classification accuracy of 90.9% with a specificity of 94.74% across 33 CT scans.

Rao et al. demonstrated a 76% classification accuracy for lung cancer detection using a CNN trained with a batch size of 20 and 1,000 iterations on the LIDC-IDRI dataset [10]. Sasikala, in [11], reported a 96% classification accuracy using a CNN model on 100 LUNG CANCER images with a resolution of 20×20 pixels. Abdul found that classifying lung CT images achieved an accuracy rate of 97.2% when utilizing a 28×28 nodule image size acquired from LIDC-IDRI [32]. Bhat et al. showcased a 96.6% accuracy rate employing CNN for categorizing 40×40 pixel LIDC-IDRI lung CT images using three convolution blocks, outperforming conventional methods [33].

Utilizing deep learning methodologies can significantly enhance both the accuracy of early detection and the automation of initial diagnoses in medical scans. This study aims to develop a robust lung cancer classification model capable of distinguishing between healthy and malignant lung CT images sourced from the LIDC-IDRI database [26]. Unlike previous studies such as [25]-[28], which focused on excised nodules, we utilized CT scans with a resolution of 512×512 pixels for this investigation. Our experiments involve the use of support vector machine (SVM) and deep convolutional neural network (CNN) classifiers to ascertain the most effective model. The SVM classifier is employed to categorize lung CT images as benign or malignant based on statistical features extracted from preprocessed LUNG CANCER CT images. Alternatively, deep learning approaches utilizing CNNs with a



single convolution block are employed for lung CT image classification. Remarkably, testing the deep CNN model on 25 test images with a resolution of 512×512 pixels resulted in a remarkable classification accuracy of 100%.

THEORETICAL BACKGROUND

This section gives a brief overview of the two classifiers used in this paper: deep Convolutional Neural Network (CNN) and Support Vector Machine (SVM). When it comes to two-class classification problems, SVM is generally considered the best tool to solve. In contrast, CNN shows no signs of being impacted by shift or spatial variance.

SVM

Support Vector Machines (SVMs) are utilized for two-class classification tasks, separating data points into distinct categories. SVM calculates a hyperplane that effectively separates these categories. In two-dimensional space, this hyperplane divides the plane into two categories or halves. By employing a discriminative classifier, SVM determines the hyperplane, where each component's estimation signifies the prediction of a different class, and each data point is represented as a point in n-dimensional space. During the training phase with labelled samples, the SVM algorithm identifies the optimal hyperplane. SVM data points encompass properties derived from the gray level cooccurrence matrix of CT images, including contrast, entropy, correlation, and homogeneity energy, as denoted in equations (1)–(4). Here, variables $P(i, j)$ represent the cooccurrence values of two pixels at coordinates (i, j) , N signifies the number of occurrence pairings, μ represents the mean, σ denotes the standard deviation, and σ^2 represents the variance. Correlation measures the degree of connectivity between each pixel and its neighbours across the entire image. A correlation value of 1 or -1 indicates a completely positive or negative correlation within the image.

Homogeneity:

Homogeneity measures the closeness of a gray level co-occurrence matrix (GLCM) element to the diagonal elements. It is computed as

$$\sum_{i,j=0}^{N-1} \frac{P_{i,j}}{1 + (i - j)^2}$$

Energy: Energy represents the sum of squared elements in the GLCM. It is also known as energy homogeneity or energy uniformity. Energy is calculated as:

$$\sum_{i,j=0}^{N-1} (P_{i,j})^2$$

Entropy:

Entropy is a metric of randomness and attains its maximum value when all elements are equal. The entropy equation is:

$$-\sum_{i,j=0}^{N-1} \ln (P_{i,j})P_{i,j}$$



Contrast:

Contrast measures local variations in the GLCM and is computed as:

$$\sum_{i,j=0}^{N-1} (i - j)^2 \cdot P_{i,j}$$

CNN

Properties such as invariance to both spatial and shift-related anomalies characterize artificial neural networks (ANNs), including convolutional neural networks (CNNs), which rely on a shared weights architecture. A CNN comprises an input layer, an output layer, and multiple hidden layers. These hidden layers commonly include convolutional, pooling, fully connected (FC), and rectified linear unit (ReLU) layers. Although the process resembles cross-correlation rather than traditional convolution, the CNN setup depends on the nature and complexity of the problem it aims to solve with the predicted output. CNNs consist of two main components: the classifier and the feature extractor. Following the convolutional and pooling layers of the feature extractor, the classification module typically incorporates zero or more FC layers. This layer determines the likelihood of the input belonging to one of the classifications. Transforming a CNN into a feature extractor involves simply removing the output layer and optionally, any remaining fully connected layers.

2.3. CNN architecture for Lung cancer detection

Layers such as the image input, convolution, ReLu, max pooling, fully connected, and softmax layers make up the architecture of CNN in lung cancer detection systems. Figure 1 illustrates this. When it comes to lung CT pictures, the categorization layer is set up with two categories: non-cancerous and cancerous. The CNN's input layer contains 512×512 pixel-sized CT images of the lungs.

The first input layer uses the LIDC-IDRI data set as input images.

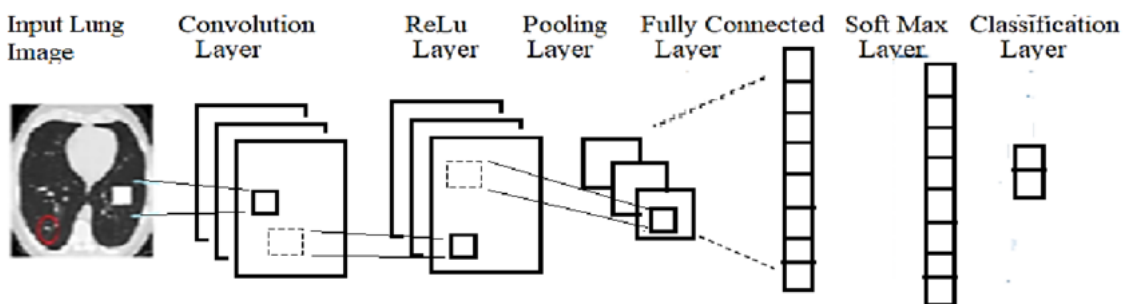


Figure 1. Layered architecture of CNN network

Within a convolutional neural network (CNN), the second layer is the convolution layer. Sliding convolutional kernels traverse the whole input picture in two dimensions in the two-dimensional convolutional layer, processing information as it goes. Incorporating a bias term into the dot product of the input and weights, this layer performs convolution. It is mathematically represented as follows:



In a convolutional neural network (CNN), the second layer is the convolution layer. Sliding convolutional kernels traverse the input picture horizontally and vertically to operate the 2-D convolutional layer. The layer incorporates a bias factor and convolves the filter with input by computing the dot product of the weights and input. Using the filter $K(m, n)$, the convolution process on the image $I(a, b)$ is depicted as follows.

$$s(t) = \sum_{a=0}^{m-1} \sum_{b=0}^{n-1} I(a, b) \cdot K(m-a, n-b) \cdot a \cdot b$$

A Max pooling layer follows the ReLU layer in a convolutional neural network (CNN) design. This layer helps to decrease the image's size by maintaining the maximum value in each 2×2 non-overlapping matrix of a single slice. Therefore, max pooling aids in keeping the most powerful activations and rejecting the rest.

Following the pooling layer in the CNN architecture, the subsequent component is the fully connected (FC) layer. In this layer, each neuron is connected to every neuron in the preceding layer, determining the likelihood score for categorization. Therefore, the FC layers in deep neural networks (DNNs) address the challenge of high-level reasoning. Preceding the final FC layer, a softmax layer is typically employed in classification tasks. This layer utilizes the softmax function to convert K real input vectors into probabilities, thereby normalizing the data. Larger input components are assigned higher probabilities. The softmax layer takes the unnormalized outputs from the network and maps them onto a probability distribution for the projected output class. Finally, the classification layers constitute the last component of deep convolutional neural network architectures. For tasks involving multiple classes, these layers compute the cross-entropy loss, assigning inputs to the predetermined number of classes based on the outputs from the preceding layer.

3. METHOD

To implement SVM and CNN, the Lung cancer recognition system is accomplished using MATLAB's neural network (NN) toolbox. As a resource for this study, the Cancer Imaging Archive public access community made available the LIDC-IDRI database, which contains images of lung cancer [29]. Over 1,200 people with various cancers affecting various body parts make up this massive dataset. The data collection for our experiments is limited to CT images containing lung cancer. Lung cancer photos, both normal and pathological, are selected from the LIDC-IDRI database. A normal lung CT scan and a cancer CT image are shown in Figure 2.

Two approaches have been utilized for the classification of lung CT images: a) a support vector machine classifier and b) a deep learning procedure based on convolutional neural networks. Using the LIDC database, 45 labelled CT images of the lungs were acquired, each with dimensions of 512×512 pixels. The presence or absence of cancer is indicated for every medical dataset. Ct scans of the lung for cancer are divided into two categories in the database: training and testing.

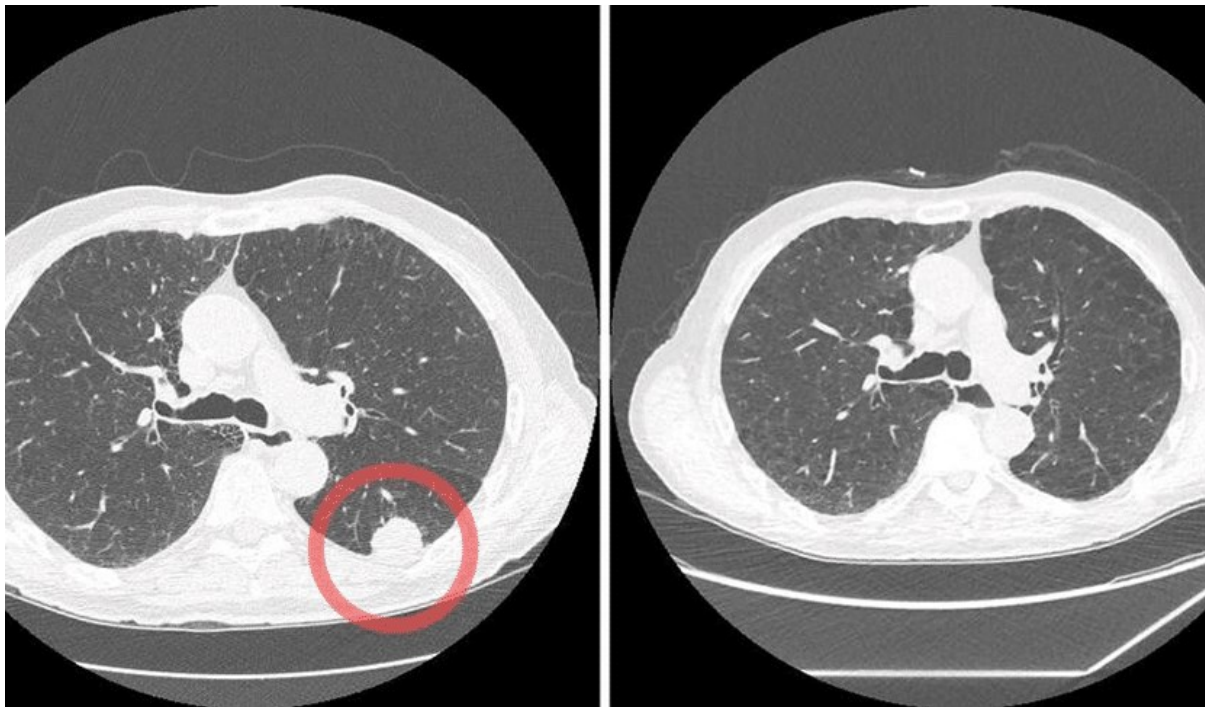


Figure 2. Lung CT scan images for, (a) Cancer and (b) Cancer

Figure 3 shows the block diagram of the Lung Cancer Detection System, which was developed and put into action. Before being fed into SVM and CNN, the input CT images undergo pre-processing that changes them from RGB to grey and finally black and white. The two methods divide CT scans of the lungs into two categories: those showing no malignancy and those showing cancer. In support vector machine (SVM) classification, features including energy, contrast, correlation, and entropy are used as inputs. These features are retrieved from a cooccurrence matrix that is generated from pre-processed 512×512 pixels size lung CT images.

The deep convolutional neural network (CNN) approach uses pre-processed pulmonary computed tomography (CT) data for both training and testing. Convolutional neural networks (CNNs) can be trained with either a single or numerous batches of randomly chosen images. Twenty CT pictures were utilized for training and ten for testing in a single batch of training, with fifteen more images set aside to evaluate classification robustness. There were three batches of twenty CT images each in the multiple batch training. There are only ever going to be two categories in the output layer: benign and malignant.

The implemented convolutional neural network (CNN) has seven layers of architecture, as shown in Figure 1. Training a convolutional neural network (CNN) involves experimenting with settings including learning rate, maximum number of epochs, momentum of learning, number of filters/kernel, and kernel size, alongside randomly initializing the weights. Before training begins, the parameters of each layer in the planned CNN network are established to allow for the analysis of parameter effects.

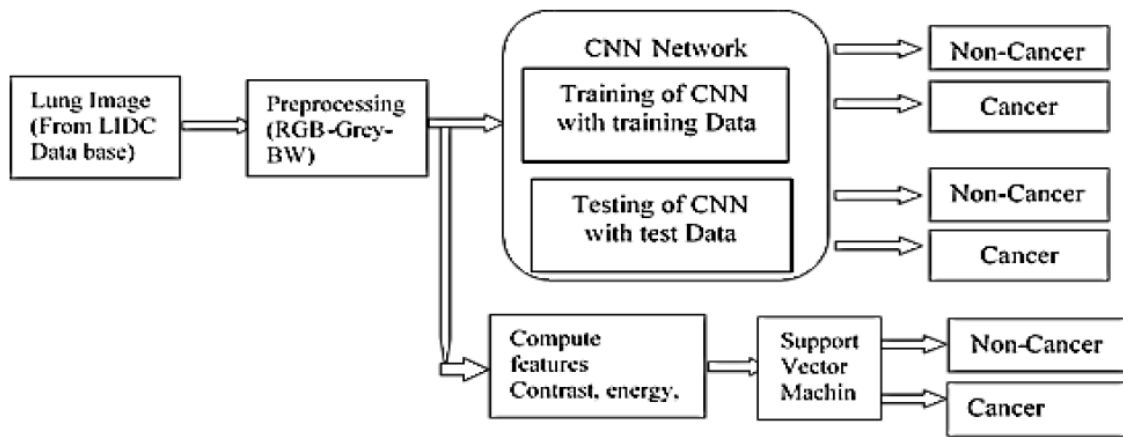


Figure 3. Shows the block diagram of the proposed LCDS

RESULTS AND DISCUSSION

There are three distinct phases to the lung cancer detection experiment: the support vector machine (SVM) phase, the convolutional neural network (CNN) phase, and the single batch training phase. We go on to talk about the results tables and the quantitative examination of these numbers. Subsections 4.1, 4.2, and 4.3 provide the relevant details. The values "1" and "0" here represent CT scans of the lung that show cancer and normal tissue, respectively.

4.1. Lung Cancer Detection using SVM

The accuracy of SVM for different input features selected is shown in Table 1. When looking at energy, correlation, or homogeneity as individual features, the SVM classifier had an accuracy of 60%; when looking at contrast, the accuracy was 65%. Here, the incorrectly identified lung cancer picture is bolded in the column containing the actual output. As an example, the value 0 in bold indicates a normal CT scan that has been labelled as a cancer imaging. More research into deep CCN is conducted due to the poor accuracy that has been achieved.

Table 1. Results of applying SVM for selected input features with 1-abnormal CT, 0-normal CT

Results of SVM with selected input features a) Energy, b) Correlation and c) Homogeneity (Kernel Function: linear)								
No. of Images	Input Image	Input Feature	Actual Output 1 or 0	Desired Output 1 or 0	Accuracy	PR	PR	Time in Seconds
20	0,1,0,1,0,1,0,1,	Energy /Correlation/H omogeneity	1,0,1,0,0,0,0,	0,1,0,1,0,1,0,1,0	60 %	60 %	40 %	2.93
	0,1,0,1,0,1,0,		0,0,0,0,1,1,0,	,1, 0,1,0,1,0,				
	1,0,1,0,1		0,1,0,0,0,0	1,0,1,0,1				
20	0,1,0,1,0,1,0,1,	Contrast	0,0,0,0,0,0,0,	0,1,0,1,0,1,0,1,0	65 %	65 %	35 %	2.511
	0,1,0,1,0,1,0,		0,0,1,0,0,0,1,	,1,0,1,0,1,0,1,0,				
	1,0,1,0,1		0,0,0,1,0,0	1,0,1				

4.2 Lung Cancer Detection training with deep convolutional neural networks utilizing different batch techniques

Multiple batch training provides flexibility and enhances accuracy when training a CNN with a big amount of database. Here, the first batch uses randomly generated convolution layer weights for initialization, while subsequent batches use the updated weights from the



preceding batch. The acquired accuracy rates are 70% for batch 1, 80% for batch 2, and 80% for batch 3 training, respectively.

4.3 Lung Cancer Detection utilizing convolutional neural networks (CNNs) with a single batch training

The suggested convolutional neural network (CNN) was trained using a training set of twenty CT pictures, ten of which were of normal lungs and ten of which were of lung cancer. Various CT scans of the lungs, some normal and some pathological, serve as the training images. Two sections make up the result analysis: a) The outcomes of the training process; b) the findings of the testing process; and accordingly.

4.3.1. Evaluation of training results

Twenty CT scans of the lungs were extracted from the LIDC database for the purpose of training. When training a CNN, it is common practice to hold constant the number of filters, pool size, and kernel size while adjusting the following parameters: a) momentum, b) starting learning rate, and c) maximum epochs. Tables 2–4 showcase the CNN accuracy as a function of a) momentum, b) initial learning rate (LR), and c) kernel size, in that order. Results from training tables 2 and 3 show that with a momentum value of 0.9 and a learning rate value of 0.01 in 68.41 seconds, CNN training achieved 100% accuracy.

Table 2. Accuracy result for varying momentum

Parameter values (const.): Initial Learning rate = 0.01, Max. epochs = 30, Kernel size = 5×5, No. of filters/kernels = 20.			
Sr. No.	Momentum	Accuracy	Time in Seconds
1	0.01	100 %	83.19
2	0.8	100 %	55.78
3	0.9	100 %	57.01

Table 3. Accuracy result for varying learning rate values

Parameter values (const.): Momentum = 0.9, Max. epochs = 30, Kernel size = 5×5, No. of filters/kernels = 20.			
Sr. No.	Initial Learning Rate	Accuracy	Time in seconds
1	0.001	100 %	68.93
2	0.01	100 %	68.41
3	0.1	50 %	61.50
4	0.2	50 %	57.29

In order to determine the optimal kernel size, the results of the training experiments are shown in Table 4. Among the tested kernel sizes (3×3, 5×5, and 9×9), the 3×3 kernel size yielded training results that were 100% correct in 39.96 seconds. There is a 100% success rate while training with epochs of 5, 10, 20, and 30. Nevertheless, for the sake of future experiments, a conservative value of 30 epochs is used.



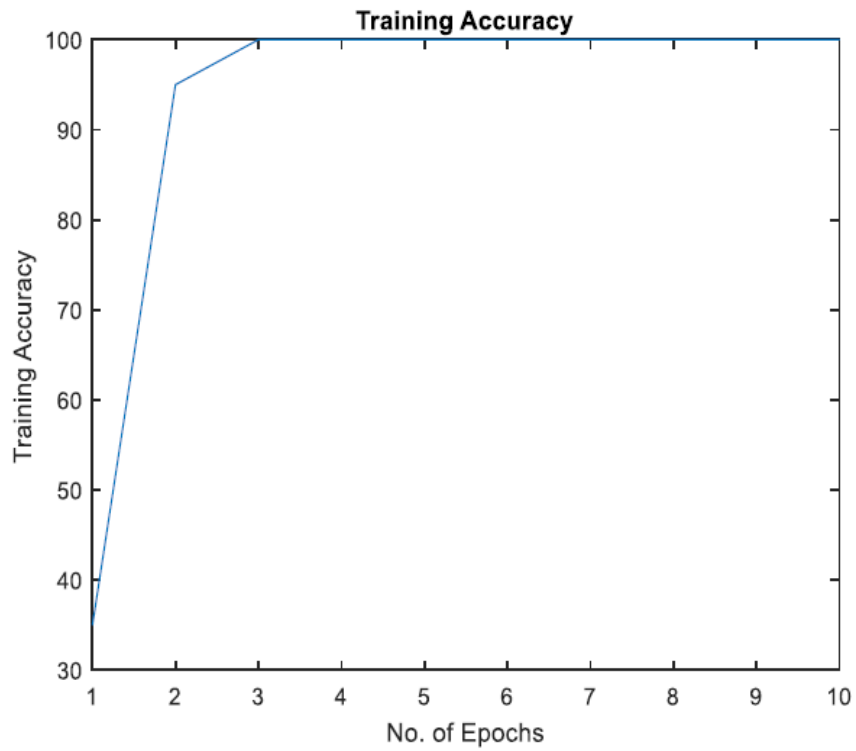
Table 4. Analysis of accuracy of training for different kernel sizes

Parameter values: Momentum = 0.9, Initial Learning rate = 0.01, Max. epochs = 30, No. of filters/kernels = 20, Stride = 2×2								
No. of images	Input Image	Kernel Size(s)	Actual Output (1 or 0)	Desired Output (1 or 0)	Accuracy	TPR	FPR	Time elapsed sec
20	0,1,0,1,0,1,0,1,0,1,	5×5 &	0,1,0,1,0,1,0,	0,1,0,1,0,1,0,1,0,	100 %	100 %	0%	40.175/39.96
	0,1,0,1,0,1,0,1,0,1		1,0,1,0,1,0,1,	1,0,1,0,1,0,1,0,				
20	1,0,1,0,1,0,1,0,1,0,	3×3	0,1,0,1,0,1	1,0,1	90 %	90%	10%	47.13
		9×9	1,0,1,0,1,0,1,	1,0,1,0,1,0,1,0,1,				
			0,1,0,1,0,1,0,	0,1,0,1,0,1,0,				
	1,0,1,0,1,0,1,0,1,0		1,0,0,0,1,0	1,0,1,0				

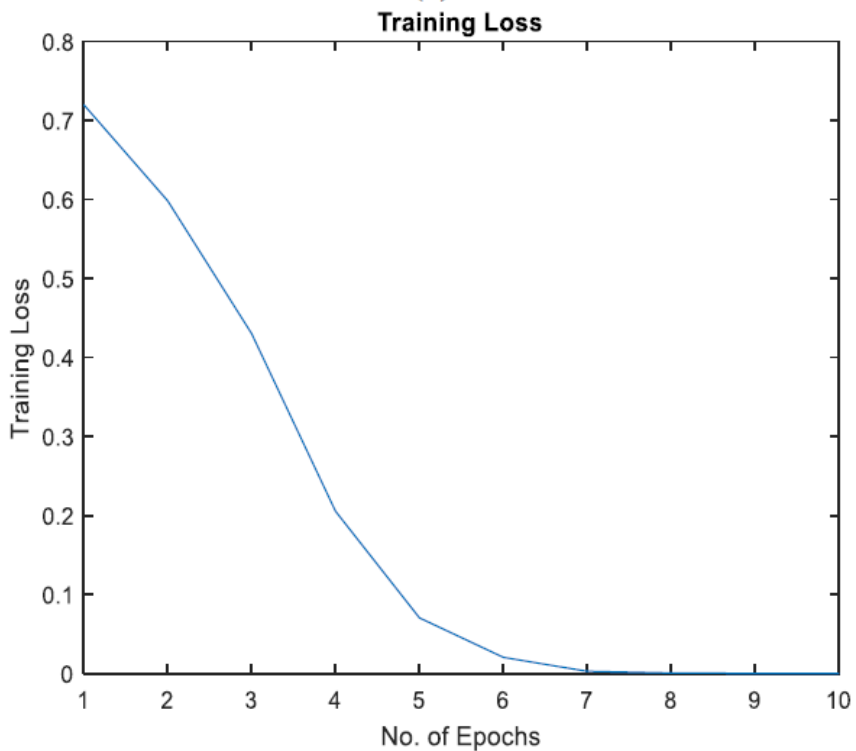
According to the study's findings, the optimal training parameters comprise a convolution layer equipped with 20 filters, each having a 5×5 filter size, a learning rate set at 0.01 with 0.9 momentum, a pool dimension of 2, a stride of 2×2, a maximum of 30 epochs, and a fully connected layer designed to output two classes: non-cancerous and cancerous. These parameters are employed for further experimental investigation. The appendix contains two graphs illustrating the outcomes: one demonstrates the training accuracy plotted against the number of epochs, while the other displays the training loss against the number of epochs. Notably, the results were obtained after approximately 5 or 8 epochs, respectively.

4.3.2: Analyzing Test Results

The optimal CNN settings were maintained during the two-cycle testing process, which used 10 and 15 lung CT images, respectively. Table 5 shows the accuracy of the CNN network's detection for the test database, along with estimates of the calculation time. Among the testing accuracy results achieved with different kernel sizes, the 3×3 kernel size demonstrated its effectiveness by yielding 100% testing accuracy in 0.944 seconds. The testing CNN network's performance is shown in Figure 5's confusion matrix. For Test data set I, the confusion matrix in Figure 5(a) shows 100% accuracy in classification, and for Data set II, it is shown in Figure 5(b). The various classification algorithms that were used are displayed in Table 6. Among the methods tested, CNN with single batch training achieved the best results, while SVM had the lowest accuracy at 60%. According to Table 7, the proposed CNN model outperforms the current state-of-the-art made by other researchers.



(a)



(b)

Figure 4. Plot of training (a) loss v/s number of epochs and (b) accuracy v/s number of epochs



Table 5. Testing accuracy of LCD with respect to the different kernel sizes

Set Parameter values: Momentum = 0.9, Initial Learning rate = 0.01, Max. epochs = 30, No. of filter = 20, Stride = 2×2									
Test Cycle	No. of Images	Input Test Image	Kernel Size(s)	Actual Output 1 or 0	Desired Output 1 or 0	Accuracy	TPR	FPR	Time seconds
I	10	1,0,0,0,1, 1,1,0,1,0	5×5 /3×3	1,0,0,0,1 .1,1,0,1,0	1,0,0,0,1, 1,1,0,1,0	100%	100%	0%	1.999 /0.944
II	15	1,1,1,1,1, 1,1,1,1,1, 1,1,1,1,1	3×3	1,1,1,1,1, 1,1,1,1,1, 1,1,1,1,1	1,1,1,1,1, 1,1,1,1,1, 1,1,1,1,1	100%	100%	0%	1.5



Figure 5. The confusion matrix result for testing with test data, (a) set I and (b) set II

Table 6. Comparison of different classification algorithms

Sr. No	Classifier	Input Feature/Batch training	Accuracy in %	TPR in %	FPR in %	Time elapsed in secs
1	SVM	Energy or Correlation or Homogeneity/--	60	60	40	2.93
2		Contrast	65	65	35	2.511
3	CNN	-/Batch-1	40	70	30	40.03
4		-/Batch-2	80	80	20	40.21
5		-/Batch-3	80	80	20	40.134
6	CNN	I-Single Batch	100	100	0	1.26
		II-Single Batch	100	100	0	2.5

Table 7. Comparison of proposed work with state-of art of research

Research Reference	Dataset /batch size/image size/learning rate/No. of Images/Conv layers	No. of Samples	Accuracy. (%)	Specificity. (%)	Sensitivity. (%)
[28]	LIDC-IDRI/-/- /-	33	90.91	94.74	85.71
[30]	LIDC/ 20/128×128/0.001/71/2	71	76	-	-
[31]	LIDC/100/20×20 pixels/0.0001/3	100	96	1	0.875
[32]	LIDC/30/28×28/833/0.01/2	8296	97.2	95.6	96.1
[33]	LIDC-IDRI /100/888/40×40 /0.01/3	2948	96.6	FPR-0.018	ERR-0.034
Proposed Work	LIDC-IDRI /multi-20 & Single /512×512/0.01/ 25/1	45	100	0	TPR-100



CONCLUSION

CNN-assisted deep learning technique has been introduced that can categorize jpeg lung CT pictures with a resolution of 512×512 pixels as either non-cancerous or malignant. Color CT scans of the lungs are first greyscale and subsequently transformed to black and white in preparation for analysis. Twenty CT scans were utilized for the training set, whereas ten (normal plus abnormal) out of fifteen images were used for testing. Both a support vector machine (SVM) classifier and a convolutional neural network (CNN) trained with numerous batches and a single batch are detailed here. Our method is superior to the state-of-the-art work of earlier researchers since our CNN approach with single batch training achieved 100% accuracy in lung cancer diagnosis in less time than the other way. As a result, we can say with confidence that CNN-based deep learning can automate the early detection of lung cancer using CT scans of the lung. Potential future work includes measuring nodule size for Lung cancer image categorization as (i) unknown, (ii) benign, (iii) malignant, or (iv) metastatic cancer, as well as evaluating the developed CNN on a larger number of Lung Cancer CT images to prove its robustness.

References

- [1] R. L. Siegel, K. D. Miller, H. E. Fuchs, and A. Jemal, "Cancer statistics, 2022," *CA: A Cancer Journal for Clinicians*, vol. 72, no. 1, pp. 7–33, 2022, doi: 10.3322/caac.21708.
- [2] N. Singh et al., "Lung Cancer in India," *Journal of Thoracic Oncology*, vol. 16, no. 8, pp. 1250–1266, 2021, doi: 10.1016/j.jtho.2021.02.004.
- [3] F. M. Sullivan et al., "Detection in blood of autoantibodies to tumour antigens as a case-finding method in lung cancer using the EarlyCDT®-Lung Test (ECLS): Study protocol for a randomized controlled trial," *BMC Cancer*, vol. 17, no. 1, 2017, doi: 10.1186/s12885-017-3175-y.
- [4] S. Ibrahim, N. Amirah Zulkifli, N. Sabri, A. Amilah Shari, and M. R. M. Noordin, "Rice grain classification using multi-class support vector machine (SVM)," *IAES International Journal of Artificial Intelligence (IJ-AI)*, vol. 8, no. 3, p. 215, Dec. 2019, doi: 10.11591/ijai.v8.i3.pp215-220.
- [5] A. Shmilovici, O. Maimon, and L. Rokach, "Data mining and knowledge discovery handbook," in Springer, O. Maimon and L. Rokach, Eds. Boston, MA: Springer US, 2009.
- [6] K. S. Parikh and T. P. Shah, "Support vector machine – a large margin classifier to diagnose skin illnesses," *Procedia Technology*, vol. 23, pp. 369–375, 2016, doi: 10.1016/j.protcy.2016.03.039.
- [7] B. H. Menze et al., "The multimodal brain tumor image segmentation benchmark (BRATS)," *IEEE Transactions on Medical Imaging*, vol. 34, no. 10, pp. 1993–2024, 2015, doi: 10.1109/TMI.2014.2377694.
- [8] Y. Pan et al., "Brain tumor grading based on Neural Networks and Convolutional Neural Networks," *Proceedings of the Annual International Conference of the IEEE Engineering in Medicine and Biology Society, EMBS*, vol. 2015-Novem, pp. 699–702, 2015, doi: 10.1109/EMBC.2015.7318458.
- [9] W. Shen, M. Zhou, F. Yang, C. Yang, and J. Tian, "Multi-scale convolutional neural networks for lung nodule classification," *Lecture Notes in Computer Science (including subseries Lecture Notes in Artificial Intelligence and Lecture Notes in Bioinformatics)*, vol. 9123, pp. 588–599, 2015, doi: 10.1007/978-3-319-19992-4_46.
- [10] G. Carneiro, J. Nascimento, and A. P. Bradley, "Unregistered multiview mammogram analysis with pre-trained deep learning models," *Lecture Notes in Computer Science*



(including subseries Lecture Notes in Artificial Intelligence and Lecture Notes in Bioinformatics), vol. 9351, pp. 652–660, 2015, doi: 10.1007/978-3-319-24574-4_78.

[11] J. M. Wolterink, T. Leiner, B. D. de Vos, R. W. van Hamersvelt, M. A. Viergever, and I. Išgum, “Automatic coronary artery calcium scoring in cardiac CT angiography using paired convolutional neural networks,” *Medical Image Analysis*, vol. 34, pp. 123–136, 2016, doi: 10.1016/j.media.2016.04.004.

[12] T. Schlegl, J. Ofner, and G. Langs, “Unsupervised pre-training across image domains improves lung tissue classification,” *Lecture Notes in Computer Science (including subseries Lecture Notes in Artificial Intelligence and Lecture Notes in Bioinformatics)*, vol. 8848, pp. 82–93, 2014, doi: 10.1007/978-3-319-13972-2_8.

[13] J. Hofmanninger and G. Langs, “Mapping visual features to semantic profiles for retrieval in medical imaging,” *Proceedings of the IEEE Computer Society Conference on Computer Vision and Pattern Recognition*, vol. 07-12-June, pp. 457–465, 2015, doi: 10.1109/CVPR.2015.7298643.

[14] G. Carneiro and J. C. Nascimento, “Combining multiple dynamic models and deep learning architectures for tracking the left ventricle endocardium in ultrasound data,” *IEEE Transactions on Pattern Analysis and Machine Intelligence*, vol. 35, no. 11, pp. 2592–2607, 2013, doi: 10.1109/TPAMI.2013.96.

[15] R. Li et al., “Deep learning based imaging data completion for improved brain disease diagnosis,” *Lecture Notes in Computer Science (including subseries Lecture Notes in Artificial Intelligence and Lecture Notes in Bioinformatics)*, vol. 8675 LNCS, no. PART 3, pp. 305–312, 2014, doi: 10.1007/978-3-319-10443-0_39.

[16] A. Barbu, M. Suehling, Xun Xu, D. Liu, S. K. Zhou, and D. Comaniciu, “Automatic Detection and Segmentation of Lymph Nodes From CT Data,” *IEEE Transactions on Medical Imaging*, vol. 31, no. 2, pp. 240–250, Feb. 2012, doi: 10.1109/TMI.2011.2168234.

[17] J. Feulner, S. Kevin Zhou, M. Hammon, J. Hornegger, and D. Comaniciu, “Lymph node detection and segmentation in chest CT data using discriminative learning and a spatial prior,” *Medical Image Analysis*, vol. 17, no. 2, pp. 254–270, 2013, doi: 10.1016/j.media.2012.11.001.

[18] L. Lu, P. Devarakota, S. Vikal, D. Wu, Y. Zheng, and M. Wolf, “Computer aided diagnosis using multilevel image features on large-scale evaluation,” *Lecture Notes in Computer Science (including subseries Lecture Notes in Artificial Intelligence and Lecture Notes in Bioinformatics)*, vol. 8331 LNCS, pp. 161–174, 2014, doi: 10.1007/978-3-319-05530-5_16.

[19] L. Lu, J. Bi, M. Wolf, and M. Salganicoff, “Effective 3D object detection and regression using probabilistic segmentation features in CT images,” *Proceedings of the IEEE Computer Society Conference on Computer Vision and Pattern Recognition*, pp. 1049–1056, 2011, doi: 10.1109/CVPR.2011.5995359.

[20] A. M. Rossetto and W. Zhou, “Deep learning for categorization of lung cancer CT images,” *Proceedings - 2017 IEEE 2nd International Conference on Connected Health: Applications, Systems and Engineering Technologies, CHASE 2017*, pp. 272–273, 2017, doi: 10.1109/CHASE.2017.98.

[21] H. Yang, H. Yu, and G. Wang, “Deep learning for the classification of lung nodules,” 2016.

[22] Q. Wu and W. Zhao, “Small-cell lung cancer detection using a supervised machine learning algorithm,” *Proceedings - 2017 International Symposium on Computer Science and Intelligent Controls, ISCSIC 2017*, vol. 2018-Febru, pp. 88–91, 2018, doi: 10.1109/ISCSIC.2017.22.



- [23] S. Kaur, “Comparative study review on lung cancer detection using neural network and clustering algorithm,” *IJARECE Journal*, vol. 4, no. 2, pp. 169–174, 2015.
- [24] F. Taher and R. Sammouda. "Artificial neural network and fuzzy clustering methods in segmenting sputum color images for lung cancer diagnosis." In *Image and Signal Processing: 4th International Conference, ICISP 2010, Trois-Rivières, QC, Canada, June 30-July 2, 2010. Proceedings 4*, pp. 513-520. 2010.
- [25] I. on Kaggle and M. Competition, “Deep learning improves cervical cancer accuracy by 81%, using intel technology,” December 22, 2017.
- [26] R. Turkki, N. Linder, P. E. Kovanen, T. Pellinen, and J. Lundin, “Antibody-supervised deep learning for quantification of tumor-infiltrating immune cells in hematoxylin and eosin stained breast cancer samples,” *Journal of Pathology Informatics*, vol. 7, no. 1, 2016, doi: 10.4103/2153-3539.189703.
- [27] H. C. Shin et al., “Deep convolutional neural networks for computer-aided detection: CNN architectures, dataset characteristics and transfer learning,” *IEEE Transactions on Medical Imaging*, vol. 35, no. 5, pp. 1285–1298, 2016, doi: 10.1109/TMI.2016.2528162.
- [28] H. Krewer et al., “Effect of texture features in computer aided diagnosis of pulmonary nodules in low-dose computed tomography,” *Proceedings - 2013 IEEE International Conference on Systems, Man, and Cybernetics, SMC 2013*, pp. 3887–3891, 2013, doi: 10.1109/SMC.2013.663.